Kinetics and Mechanism of the Reaction between an Arenediazonium Ion and Methyl Gallate (= Methyl 3,4,5-Trihydroxybenzoate) in Aqueous Solution: Evidence for Diazo Ether Formation through an O-Coupling Reaction

by **Sonia Losada-Barreiro**, **Verónica Sánchez-Paz**, **Carlos Bravo-Díaz***

Universidad de Vigo, Facultad de Química, Dpt. Química Física, E-36200 Vigo
(phone: +34 986 812303; fax: 34 986 812556; e-mail:cbravo@uvigo.es)

We have investigated the kinetics and mechanism of the reaction between 3-methylbenzenediazonium ions (3MBD) and methyl gallate (= methyl 3,4,5-trihydroxybenzoate; MG), in aqueous buffer solution by employing spectrophotometric (UV/VIS) and electrochemical (linear-sweep voltammetry, LSV) techniques and computational methods. Because the absorption band of MG overlaps that of 3MBD, the reaction was monitored spectrophotometrically by measuring the changes in absorbance with time due to product formation, and biphasic kinetic profiles, indicative of accumulation of an intermediate in the course of the reaction, were obtained. The formation of an intermediate was confirmed by LSV. The observed rate constants k_{obs} for 3MBD disappearance were obtained by fitting the decrease in the peak current of the first reduction peak of 3MBD with time to the integrated first-order equation. The variation of k_{obs} with [MG] was determined at different pH values and follows a saturation kinetic pattern. Alternatively, at a fixed [MG], k_{obs} values show an inverse dependence on [H^+], suggesting that the reactive species is the anion and not the neutral form of MG. To discern which of the three OH groups of MG is the first one undergoing deprotonation, the geometries of the resulting anions were optimized by using B3LYP hybrid density functional theory (DFT) and a 6-31G(+ +d,p) basis set. The deprotonation energies suggest that the OH group at the 4-position is first deprotonated. The kinetic results can be accommodated, therefore, by assuming two competitive mechanisms, the spontaneous $D_N + A_N$ decomposition involving 3MBD, and a mechanism involving an electrophilic attack at the O-atom at C(4) in a pre-equilibrium step, leading to the formation of a transient diazo ether of the type Ar−N=N−O−R which further decomposes. All attempts to isolate and characterize the diazo ether failed.

Introduction. – Arenediazonium ions ArN_2^+ may show an ambivalent behavior toward electron-rich donors. On the one hand, they may function as 1-electron oxidants giving rise to different reduction products [1–7]. Alternatively, they may function readily as *Lewis* acids reacting with *Lewis* bases (nucleophiles) Nu^- or NuH (followed by loss of a proton) to give covalently bonded adducts $ArN_2−Nu$, by reaction at N(β) of the arenediazonium ion, which is the electrophilic reactive center (*Scheme 1*) [8][9].

The stability of the adduct is critically dependent on the leaving ability of the nucleophile, so that if Nu^- is a good leaving group such as halide or acetate ions, the equilibrium lies largely on the side of the reactants, and ArN_2^+ ions undergo spontaneous decomposition reactions which occur through a $D_N + A_N$ mechanism, *i.e.*, rate-limiting formation of a highly unstable aryl cation which further reacts with any nucleophile available in its solvation shell [9–11]. On the other hand, if Nu^- is a good nucleophile but a relatively poor leaving group (such as the ascorbate ion),

Scheme 1. *Basic Representation of the Spontaneous* $D_N + A_N$ *Dediazoniation Mechanism Leading to Products Ar–Nu of Heterolysis and of the Nucleophilic Addition Mechanism Leading to the Formation of Adducts in the (*E*)- and (*Z*)-Configurations*
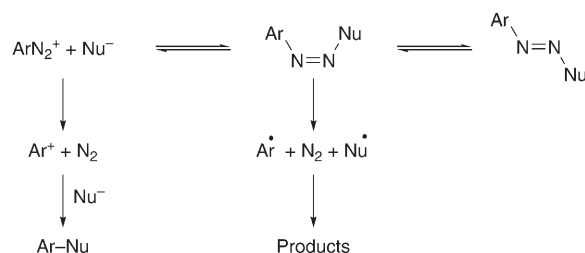
stabilization may occur by conversion to a thermodynamically stable isomer (*e.g.*, (*Z*)/(*E*) isomerization) [4][12]. In certain circumstances, isomerization is not possible and the adduct splits homolytically to finally give reduction products [13–15]. Typical examples of covalently bonded adducts are the azo dyes (C-coupling), but other atoms may be involved leading to the so-called N-, O-, S-, and P-coupling reactions [8][9].

C-Coupling reactions have been studied for over half a century, and in many aspects, they are almost ideal systems for mechanistic investigations [9][16]. Because aromatic diazonium ions are relatively weak electrophiles, they only undergo C-coupling with activated nucleophilic arenes carrying electron-releasing hydroxy, amino, or comparable functional groups; either the hydroxy or the amino group increases the C-nucleophilicity of the coupling component undergoing electrophilic aromatic substitution leading to the formation of azo dyes (*Scheme 2*) [17]. All C-coupling reactions are believed to proceed through the general electrophilic aromatic substitution (EAS) mechanism involving the formation of donor–acceptor complexes (or π-complex), **DA**, followed by the formation of a covalent (or σ) complex, the *Wheland* intermediate **W** (see *Scheme 2* [9][16][18]). From **W**, the substitution products **P** are obtained by proton loss in a step which is usually considered, for the azo coupling reaction, to be irreversible [17]. In fact, the observation of *Wheland* complexes **W** in azo coupling reactions is a rare experimental feature because these σ-complexes have not been directly observed for a long time even though they were proposed on the basis of kinetic data [8][9][18]. However, recently, *Forlani* and co-workers [19] provided NMR evidence supporting the formation of *Wheland* complexes in the course of C-coupling reactions between 4-substituted arenediazonium ions with

Scheme 2. *Basic Illustration of the Commonly Accepted Electrophilic Aromatic Substitution Mechanism Leading to the Formation of a Stable Azo Dye Through the Formation of π- and σ-Complexes.* The π-complex is not customarily detected because the formation of the σ-complex **W** is usually fast. B: any base.
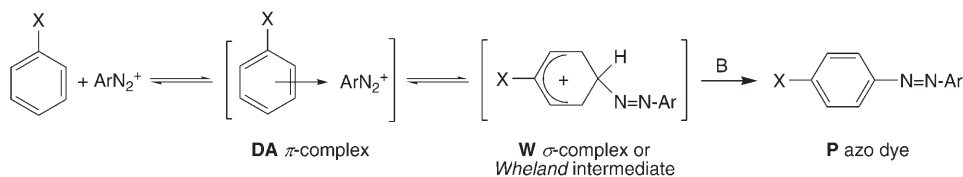
1,1′,1″-(benzene-1,3,5-triyl)tri[piperidine] and 4,4′,4″-(benzene-1,3,5-triyl)tris[morpholine].

The presence of two ionizable groups (*e.g.*, two OH groups) at the nucleophilic arene moiety increases the reactivity of the substrate, but their effect has been proved not to be additive and strongly dependent on their relative positions at the benzene ring [8][9][20]. For instance, resorcinol (= benzene-1,3-diol) has two ionized forms and has been shown as an example of a molecule having two nucleophilic centers able to couple, the dianion coupling being more than 10^4 times faster than the monoanion coupling [9][21]. In contrast, the other two dihydric phenols (= benzenediols), catechol (= benzene-1,2-diol) and hydroquinone (= benzene-1,4-diol), are oxidized in the presence of diazonium ions and can undergo coupling reactions only under strictly defined conditions, *e.g.*, by first esterifying one of the OH groups and hydrolyzing it later.

Reactions with trihydric phenols such as pyrogallol (= benzene-1,2,3-triol), phloroglucinol (= benzene-1,3,5-triol), gallic acid (= 3,4,5-trihydroxybenzoic acid) or its esters (= 3,4,5-trihydroxybenzoates) have not been explored by far as much as those of the mono- and dihydric derivatives [9], and a literature survey revealed that very few kinetic studies on their reactions with arenediazonium ions have appeared in the past. The few studies found exploit the metal-complexing properties of the trihydric phenols for analytical purposes; *e.g.*, *Zhu et al.* [22] took advantage of the reaction between 4-nitrobenzenediazonium ions with gallic acid to develop an analytical procedure for determining titanium in geochemical samples. The reaction was also exploited by *Dmitrienko* and co-workers [23] to determine gallic acid based on the solid-phase extraction of the presumed azo dye formed in the course of the reaction.

The possibility of ArN_2^+ ions undergoing O-coupling reactions with compounds bearing OH groups attracted the attention of our laboratory, and we recently showed that the reaction with ascorbic acid, a well-known reducing agent, does not proceed through the expected radical pathway but proceeds through the formation of transient diazo ethers [4–7]. Similar situations where found when reacting ArN_2^+ ions with neutral nucleophiles such as MeOH [15] and EtOH [14] and in systems of restricted geometry [13]. We are also interested in determining the distribution of polar organic molecules such as antioxidants in emulsified systems by using arenediazonium ions as chemical probes that react with a given antioxidant, the kinetic results being interpreted in terms of a pseudophase model [24][25]. Knowledge of antioxidant distribution in food emulsions is important because the efficiency of antioxidants in inhibiting lipid peroxidation depends, among others, on their distribution within the different regions of the system [25–27].

As a continuation of our investigations and to expand the current knowledge on the reactivity of arenediazonium ions with trihydric phenols, we undertook a study of the reaction between 3-methylbenzenediazonium ions (3MBD) with methyl gallate (MG) which was chosen as a model trihydric phenol because of its potential use as antioxidant or pro-oxidant [28–31]. The 3MBD was chosen because substantial knowledge on its spontaneous decomposition in aqueous acid solution is available, and because it bears an electron-donating group, which makes 3MBD less prone to react through homolytic pathways as others bearing electron-withdrawing groups such as 4-nitrobenzenediazonium ions. Its electrophilicity is high enough to be able to undergo C-coupling reactions

with naphthalenols and naphthalenamines [32][33] and O-coupling reactions with ascorbate ions in aqueous and micellar systems [4–7] and even with neutral nucleophiles such as EtOH [14].

As we will see, the kinetic results obtained are not consistent with the general C-coupling mechanism but rather provide evidence for an O-coupling reaction proceeding through the formation of an unstable diazo ether experimentally detectable, that further decomposes.

Results. – 1. *Spectroscopic Evidence for the Formation of an Unstable Intermediate during the Reaction Between 3MBD and MG. Effects of pH and [MG].* Because the absorption band of MG overlaps that of 3MBD (see *Exper. Part*), the course of the reaction between MG and 3MBD was monitored under pseudofirst-order conditions ([MG]≫[3MBD]) by measuring the changes in absorbance at λ 440 nm due to product formation. *Fig. 1,a* shows the typical absorbance–time profiles obtained at different [MG] at a fixed pH of 5 (buffer control). As illustrated, the absorbance increases rapidly with increasing [MG], up to a maximum after which a decrease is detected approaching, at high [MG], a constant value that depends on the initial [MG] employed. The maximum absorbance A_{max} increases upon increasing [MG] up to 0.03M, after which it becomes independent of [MG] (results given as supplementary material (*Fig. S1,a*)[1]). The time t_{max} at which the maximum of absorbance is reached also depends on [MG], and decreases in an exponential fashion from *ca.* 1200 s when [MG] = 0.001M up to a roughly constant value of *ca.* 350 s when [MG] = 0.1M at pH 4.5. At pH 4.3, t_{max} is *ca.* 3000 s when [MG] = 0.001 and decreases by a factor of 2 when [MG] = 0.1M (results given as supplementary material (*Fig. S1,b*)[1]). The biphasic profile obtained is, therefore, suggestive of accumulation of an intermediate which has a higher molar absorptivity than that of the final product at the employed wavelength.
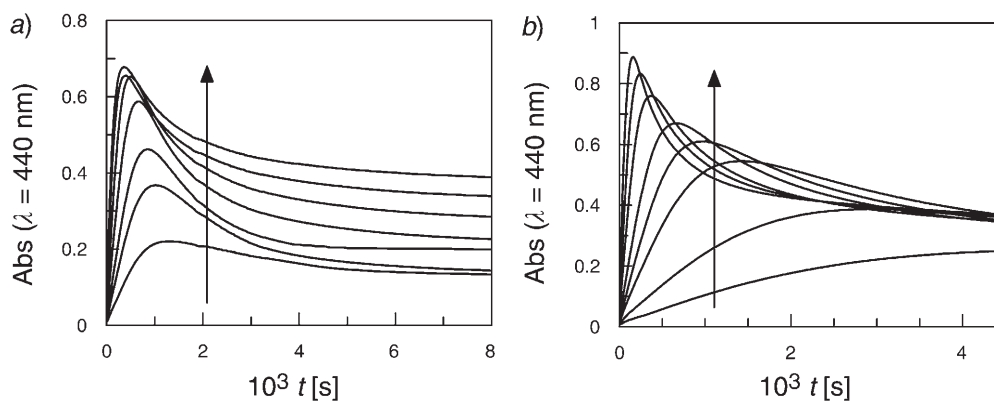

Fig. 1. *Variation in the absorbance (λ 440 nm) with time due to product formation* a) *at fixed pH 5.0 and [MG] increasing (↑) from 0.001 to 0.08M, and* b) *at fixed [MG] = 0.04M and pH increasing (↑) from 3.7 to 5.3.* [3MBD] ≈ 3·10⁻⁴ M, *T* 30°.

---

[1]   Supplementary material is available upon request from the authors.

The results also indicate an important effect of acidity on the rate of the reaction which was further investigated.

Fig. 1,b, shows the effects of acidity on k_{obs} at constant $[MG] = 0.04$M. Again, the variation of the absorbance (λ 440 nm) with time follows a biphasic profile suggestive of the formation of an intermediate. The absorbance at infinite time is independent of the pH, indicative that all starting 3MBD was transformed into products. The A_{max} values increase approximately in a linear fashion on lowering the acidity from pH 3.5 to 6.5, and the t_{max} values decrease rapidly upon lowering the acidity from *ca.* t_{max} 5000 s (pH 3.6) to t_{max} 15 s at pH 6.5, denoting the significant effect of acidity on the rate of the reaction (results given as supplementary material in (*Figs. S2,a* and *b*, resp.)[1]).

Because of the complex kinetic behavior found and wishing to further investigate the mechanism of the reaction, we decided to employ linear-sweep voltammetry (LSV) as working tool to monitor the reaction. Arenediazonium ions and some of their derivatives such as $Ar-OH$ and $Ar-N=N-Nu$ are electroactive compounds [34][35], making electrochemical methods very convenient to study the chemistry of ArN_2^+ ions. The electrochemical techniques are very sensitive (concentrations as low as 10^{-9} M can be detected) and may also show selectivity, allowing detection of unstable intermediates in the course of dediazoniations [4][5][13] and, in some instances, simultaneous monitoring of ArN_2^+ disappearance and product formation [36][37].

2. *Electrochemical Monitoring of the Reaction Between 3MBD and HG. Further Evidence for the Formation of a Transient Intermediate.* The electrochemical reduction of 3MBD shows two well-defined reduction peaks, in keeping with previous results [4][34][38]. The first one, *Fig. 2,a*, appears at E_p *ca.* -0.05 V and is associated with the transfer of one electron to yield the corresponding aryldiazenyl radical $ArN_2^{\bullet}$. The second one (not shown in *Fig. 2,a*, for the sake of clarity) appears at E_p *ca.* -1.2 V and is associated with a $3e^-/3H^+$ uptake to finally yield an arylhydrazine ($ArNHNH_2$). The peak current i_p of both reduction peaks increases linearly with [3MBD] (correlation coefficient $cc > 0.999$) up to $4 \cdot 10^{-4}$ M (results not shown).
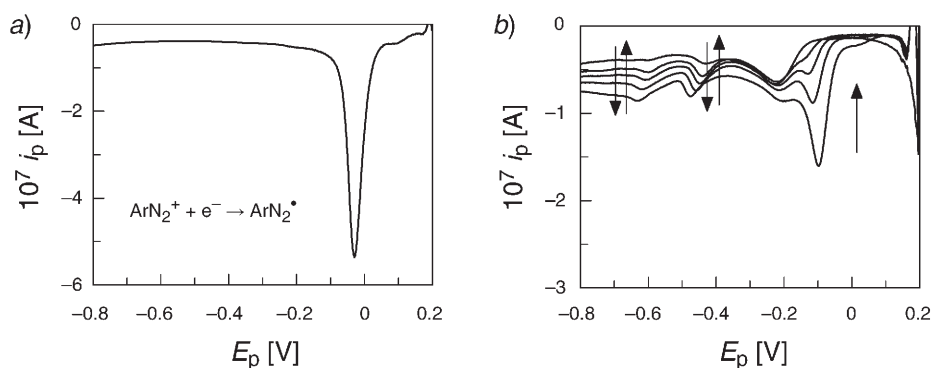

Fig. 2. a) *Voltammogram of 3MBD in aqueous solution (BR buffer) showing the first reduction peak and the associated chemical process.* b) *Representative voltammograms obtained at different times in the course of the reaction between 3MBD and MG.* The arrows indicate the observed trend in the variation of the peak currents with time. $[MG] = 0.06$M, $[3MBD] = 9.4 \cdot 10^{-5}$ M, pH 4.7, T 30°.

On addition of MG, voltammograms become more complex, and new reduction peaks appear at $E_p = -0.15$ V, E_p *ca.* -0.5 V, and $E_p = -0.64$ V, which are not detected in the absence of MG. *Fig. 2,b*, chosen as representative, shows voltammograms obtained at different times in the course of the reaction, and *Fig. 3,a*, shows the variation of i_p with time of the reduction peaks at E_p *ca.* -0.05 V, E_p *ca.* -0.5 V, and $E_p = -0.64$ V. The variation of i_p of the reduction peak at $E_p = -0.15$ V with time could not be determined accurately because it is partially overlapped with that of 3MBD ($E_p = -0.05$ V). At infinite time, *i.e.*, when the reaction is complete, only the reduction peak at $E_p = -0.15$ V is detected. It appears evident, therefore, that a transient intermediate is formed in the course of the reaction in keeping with the results obtained spectrophotometrically (*Fig. 1*). Inspection of the data in *Fig. 3,a*, reveals that the formation of the transient intermediate is faster than its decomposition, and that the maximum intermediate concentration is reached when *ca.* 70% of 3MBD has been consumed.
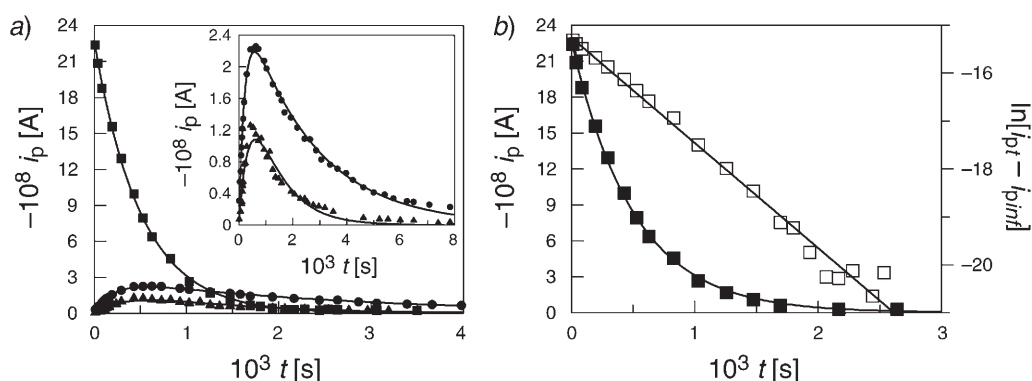

Fig. 3. a) *Variation with time of the peak currents of the reduction peaks at* $E_p = -0.05$ V (■), $E_p = -0.5$ V (●), *and* $E_p = -0.64$ V (▲). Inset: Amplification of the variation of the i_p of the reduction peaks associated with the formation and disappearance of the transient intermediate. The solid lines were drawn by fitting the exper. data to a first-order equation (3MBD loss) and to help the eye by fitting the i_p/t data for the intermediate to an equation derived from a consecutive mechanism of the type $A + B \rightarrow I \rightarrow$ products. b) *Variation of* i_p *of the peak associated to 3MBD loss* (■, $E_p = -0.05$ V) *and linear plot* (□) *according to the first-order equation.* [MG] = 0.06M, [3MBD] = $9.5 \cdot 10^{-5}$ M, pH 4.7 (*BR* buffer), *T* 30°.

Because the LSV method has been proved to be selective allowing simultaneous monitoring of 3MBD consumption and product formation (*Fig. 3,a*), the observed rate constant k_{obs} was obtained by fitting the i_p/t data for 3MBD ($E_p = -0.05$ V) to the integrated first-order equation, as shown in *Fig. 3,b*.

3. *Effects of [MG] on* k_{obs}. *Fig. 4* shows the variation of k_{obs} with [MG] following a saturation kinetics profile, suggestive of a mechanism involving a rate-determining decomposition of a transient intermediate produced in a rapid pre-equilibrium step, in keeping with spectroscopic and electrochemical experiments (*Figs. 1* and *3*). Higher MG concentrations could not be employed because of the limited MG solubility in aqueous solution [17]. *Fig. 4* shows that, in the absence of MG, $k_{obs} = (4 \pm 0.2) \cdot 10^{-4}$ s^{-1}, a value equal to that reported in the literature for the spontaneous decomposition of 3MBD [11][32][39]. When [MG] = 0.1M, k_{obs} increases by factors of *ca.* 4 (pH 4.5) and

ca. 6 (pH 4.7) with respect to the value in its absence, denoting again the significant effect of the acidity on k_{obs}, which was further investigated.
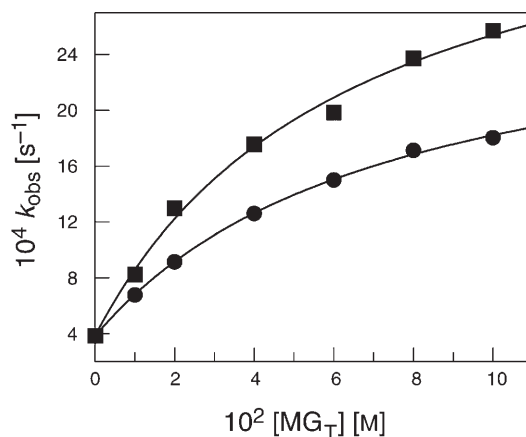

Fig. 4. *Effects of [MG] on* k$_{obs}$ *in aqueous* (buffer controlled) *solution.* ● pH 4.5, ■ pH 4.7. [3MBD] = $9.5 \cdot 10^{-5}$ M, T 30°.

4. *Effects of Acidity on* k$_{obs}$. *Fig. 5,a*, shows the effects of acidity on k_{obs}, its variation following an upward bend with k_{obs} increasing about 10 times on going from pH 4.3 up to pH 5.4. Higher acidities were not employed because reactions become too slow, with k_{obs} values approaching that for the thermal decomposition of 3MBD, $k_{obs} = (4 \pm 0.2) \times 10^{-4}$ s^{-1}, and lower acidities could not be employed because the reactions become too fast to be monitored electrochemically and to minimize MG autooxidation, which may be important in alkaline solution [40][41]. The variation of log(k_{obs}) with pH is linear (*Fig. 5,b*) with a slope of 1.03 ± 0.04, indicating an inverse dependence of k_{obs} on [H$^+$].
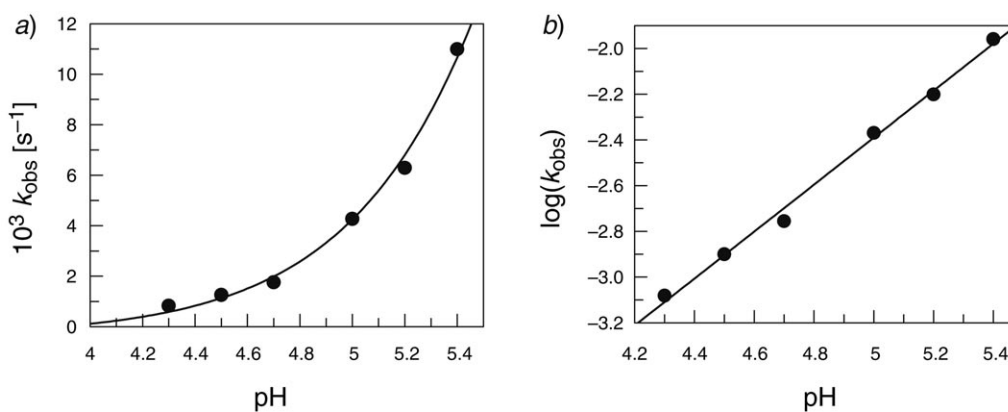

Fig. 5. a) *Variation in* k$_{obs}$ *upon changing pH showing an upward bend profile.* b) *Representation of* log(k$_{obs}$) *with pH showing a linear relationship with a slope of 1.03 ± 0.04, indicative of an inverse relationship between* k$_{obs}$ *and [H$^+$].* [3MBD] = $9.5 \cdot 10^{-5}$ M, [MG] = 0.04M, T 30°.

Auxiliary experiments (not shown) carried out with different buffer concentrations, by varying buffer nature (AcOH/AcO⁻), and by intentionally adding different amounts of a base ([pyridine] = 0.01 – 0.05M) revealed no significant changes in k_{obs}, thus suggesting that proton loss is not involved in the rate-limiting step and that the reaction is not general-base-catalyzed.

5. *Attempted Isolation of the Intermediate and Final Products*. A number of unsuccessful attempts were made to isolate the detected intermediate (see *Figs. 1* and *3*).

For this purpose, an aq. acid (pH 4.5) soln. (250 ml) containing methyl gallate (MG; 2.6 g, 0.014 mol) were mixed with an aq. acid (pH 6) soln. (100 ml) containing 3MBD (0.36 g, 0.002 mol). An orange color appeared immediately, turning to reddish with time. The reaction was allowed to proceed during the time necessary to obtain the maximum intermediate concentration (*t ca.* 7 min, estimated by employing LSV as illustrated in *Fig. 3,a*), and the formed products were immediately extracted with CH_2Cl_2 (3 × 60 ml). Column chromatography (silica-gel, activated with CH_2Cl_2/MeOH 95:5) of the extracts yielded colorless fractions and some yellow, orange, and dark red fractions. Their TLC showed several spots indicative of the presence of a variety of products making the attempts of isolation unsuccessful. Similar results were obtained when extraction was performed with solvents of different polarity such as hexane or AcOEt.

Attempts to synthesize the reaction products were also unsuccessful.

On a semi-prep. scale, MG (0.188 g, 0.001 mol) was dissolved in a slightly acid aq. soln. (10 ml; phosphate buffer control, pH 6) containing $KAl(SO_4)_2 \cdot 12 H_2O$, and the mixture was placed in an ice bath with continuous stirring. Independently, 3MBD (0.21 g, 0.001 mol) was dissolved in an aq. acid (pH 6) soln. (10 ml). The reaction was initiated by adding dropwise the 3MBD soln. to the mixture containing MG. Immediately, bubbling was detected accompanied with the formation of yellowish foam and the formation of a precipitate. The precipitate was filtered at reduced pressure and tried to recrystallize in hot EtOH, but it turned darker immediately and a tarry-like material was formed. TLC (CH_2Cl_2/MeOH 99:1) revealed the presence of several spots. Attempts to extract the products with common organic solvents such as CH_2Cl_2, hexane, or AcOEt led to the formation of intractable tarry materials, indicating that the nature of the solvent is crucial to the stability of the formed products.

Discussion. – The dependence of k_{obs} on acidity, illustrated in *Fig. 5,b*, suggests an inverse dependence of k_{obs} on [H⁺] because the plot of $\log(k_{obs})$ *vs.* pH is linear with a slope of 1.03 ± 0.04. This finding suggests that the reaction between 3MBD and MG takes place through the ionized form of MG.

Methyl gallate has three ionizable OH groups and, therefore, can exist in four different molecular forms depending on the working pH (*Scheme 3*). While the pK_{a1} and pK_{a2} values can be easily determined from potentiometric or spectrophotometric titrations, the pK_{a3} values are not known accurately because of the instability of gallates to oxidation in alkaline solution [40][41]. The first acidity constant ($pK_{a1} = 8.03$) is likely to be associated to the OH group in the 4-position (see structure **1B** in *Scheme 3*), because it allows delocalization of the negative charge and because the presence of two *ortho* OH groups stabilize the negative charge by the formation of intramolecular H-bonds (see structure **1D**). The assumption is supported by evidence from B3LYP density functional theory (DFT) calculations performed with a 6-31G(+ +d,p) basis set. A complete geometry optimization was carried out for the different anions and their energy compared to that of the parent molecule **1A**. The results show that **1D** has

an energy *ca.* 30 kJ/mol lower than that of **1E** and that the highest calculated electron density (HOMO orbital) is located on the O-atom at C(4) (see **1F**). These considerations suggest, therefore, that the reaction would not proceed through a C-coupling mechanism (*Scheme 2*) because C(1), C(3), and C(5) are blocked by the carboxylate and the OH groups and, therefore, can not be activated[2]). In addition, the saturation kinetics profile shown in *Fig. 4* is not compatible with the predictions of the EAS mechanism in *Scheme 2*, and new mechanistic alternatives need to be proposed.

Scheme 3. *Ionization of Methyl Gallate at the 4-Positon and Possible Resonance Forms* (see **1A** – **1D**) *Showing the Intramolecular Hydrogen Bonds*[a])
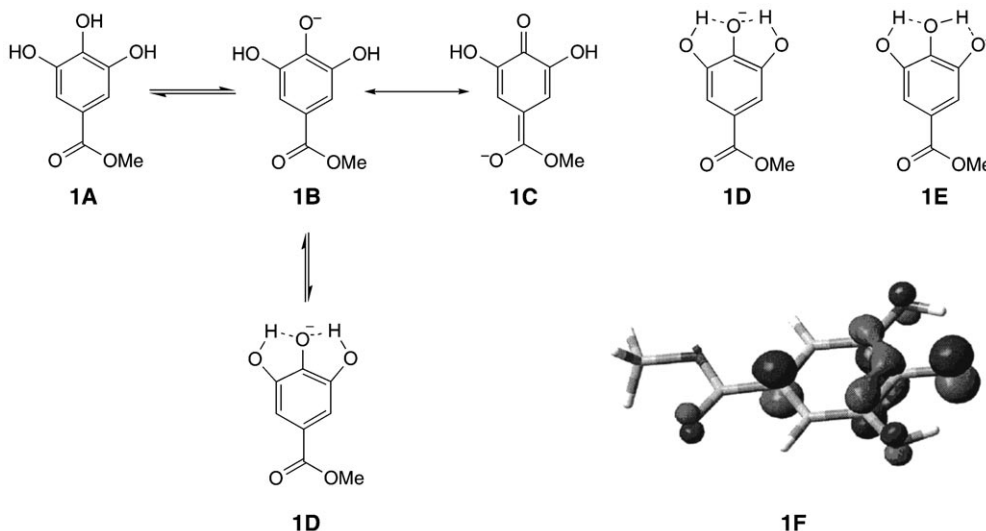

[a]) The optimized structure **1E**, showing the ionization at the 3-position, lies higher in energy than structure **1D**. The geometry of structure **1F** is the same as that of **1D** but shows the HOMO orbitals as determined by DFT theory (B3LYP, 6-31G(+ +d,p) basis set), illustrating that the highest electron density is located on the O-atom at C(4) of MG, little electron density is on the O-atoms at C(3) and C(5), and negligible electron density is at C(2) and C(6), suggesting, therefore, that an electrophilic attack is likely to take place on the O-atom at C(4) (O-coupling) rather than on the O-atoms at C(3) and C(5) or on C(2) and C(6) (C-coupling).

The collected kinetic evidence and the computational results suggest a reaction mechanism which involves an intermediate formed in equilibrium with the reactants, and where one reaction participating in the equilibrium is second-order and the equilibrium is followed by a first-order consecutive step (*Scheme 4*). Consistent with this interpretation, *Figs. 1*, *2*, and *3,a*, show the formation of an intermediate in the

---

[2]) The C-coupling reactions are probably the electrophilic aromatic substitution (EAS) reactions characterized to the highest degree by its sensitivity to orientation. In practically all cases investigated, the aromatic substrate reacts only if a strong electron donor is present, the reactivity order being $O^- > NR_2 > NHR > OR > OH \gg Me$, and the C-coupling takes place exclusively at the *o*- and *p*-positions. In fact, *m*-substitutions have never been observed.

Scheme 4. *Proposed Reaction Mechanism Between 3MBD and Methyl Gallate Comprising the Spontaneous* $D_N + A_N$ *Pathway and a Competitive Reaction Leading to the Rapid Formation of an Unstable Transient Intermediate that Further Decomposes in a Rate-Limiting Step*
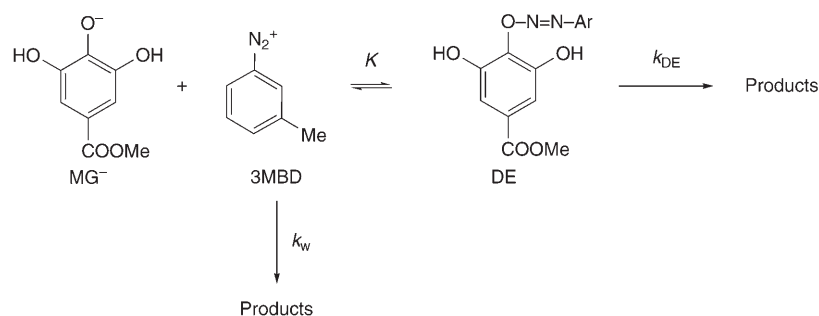
course of the reaction whose maximum concentration is reached when *ca.* 70% of the initial amount of 3MBD has been consumed.

The possibility of 3MBD undergoing O-coupling with MG is not unlikely because there exist a diversity of reactions where O-nucleophiles add to diazonium ions at $N(\beta)$ to give (*Z*)-adducts as kinetically controlled products, *i.e.*, $Ar-N=N-O-R'$ ($R' =$ alkyl, aryl) [9]. In most cases, the nucleophile must possess a charge, such as in the case of OH^-, CN^-, RO^-, or ascorbate ions, and experimental conditions are chosen so that substantial concentrations of the anionic form of the nucleophile are present [4][5][9][12]; but formation of (*Z*)-diazo ethers with neutral nucleophiles has also been reported [13 – 15]. In fact, a similar mechanism was proposed by *Luchkevitch et al.* [42] to explain the kinetic results obtained when studying the reaction between some substituted benzenediazonium ions with hydroxynaphthalenesulfonic acid derivatives.

From *Scheme 4*, the rate of 3MBD disappearance is given by *Eqn. 1*, where k_w and k_{DE} are the rate constants for the thermal decomposition of ArN_2^+ and for the unimolecular cleavage of the diazo ether, and [DE] and $[ArN_2^+]_F$ represent the formed diazo ether and the 'free' arenediazonium ion concentrations, respectively. [DE] is given by *Eqn. 2*, where K is the equilibrium constant for the formation of the adduct DE and $[ArN_2^+]_F$ the concentration of 'free' 3MBD. Substitution of *Eqn. 2* into *Eqn. 1* and taking into consideration the corresponding mass balance for ArN_2^+, the first ionization equilibrium for MG, and bearing in mind that we have worked under pseudofirst-order conditions, the observed rate constant k_{obs} is given by *Eqn. 3*. The parameter *A* is defined by *Eqn. 4*, where K_{a1} stands for the first ionization constant of MG ($pK_{a1} = 8.03$) and $[H^+]$ is the hydronium ion concentration. *Eqn. 3* is typical of a saturation kinetics profile such as that shown in *Fig. 4*, where k_{obs} becomes eventually independent of the MG concentration at high $[MG_T]$. Note that *Eqn. 3* predicts that when $[MG_T] = 0$, *i.e.*, no MG is added, the observed rate constant is equal to that for the spontaneous decomposition, $k_{obs} = k_w$, as observed in *Fig. 4*. Because the reaction in the presence of MG is faster than the spontaneous decomposition of 3MBD (*Fig. 4*), *Eqn. 3* can be reorganized to *Eqn. 5*, which predicts that, at a given $[H^+]$, a reciprocal plot of $1/k_{obs}$ *vs.* $1/[MG_T]$ should be a straight line. *Fig. 6* shows such linear plots from where the values of k_{DE} and K shown in the *Table* can be calculated ($K_a = 8.03$).
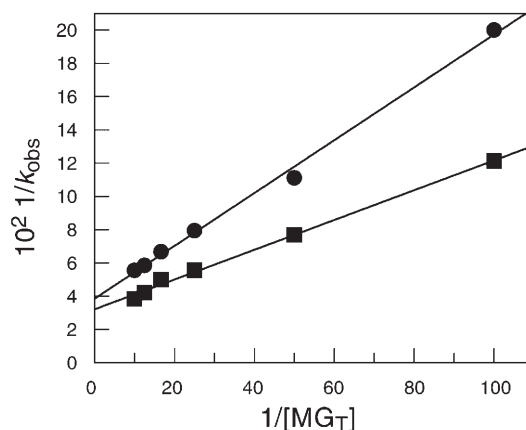
Fig. 6. *Double reciprocal plot according to* Eqn. 5

Table. *Values for the Unimolecular Decomposition Constant* k_{DE} *of the Transient Diazo Ether Formed in the Course of the Reaction, the Equilibrium Constant* K *for Diazo Ether Formation* (see *Scheme 4*) *and the Parameter* A *as Defined by Eqn. 4*

pH	$10^3\,k_{DE}/s^{-1}$	A	$10^{-4}\,K\,[\text{M}^{-1}]$
4.5	2.6 ± 0.2	24 ± 2	8.1 ± 0.7
4.7	3.1 ± 0.1	35 ± 3	7.5 ± 0.6

$$\nu = \frac{-d[\text{ArN}_2^+]}{dt} = k_w[\text{ArN}_2^+]_F + k_{DE}[\text{DE}] \qquad (1)$$

$$[\text{DE}] = K[\text{ArN}_2^+]_F[\text{MG}^-] \qquad (2)$$

$$k_{obs} = \frac{k_w + Ak_{DE}[\text{MG}_T]}{1 + A[\text{MG}_T]} \qquad (3)$$

$$A = \frac{K_{a1}K}{K_{a1} + [\text{H}^+]} \qquad (4)$$

$$\frac{1}{k_{obs}} = \frac{1}{k_{DE}} + \frac{1}{Ak_{DE}[\text{MG}_T]} \qquad (5)$$

The average k_{DE} value is $(2.9 \pm 0.1) \cdot 10^{-3}\,s^{-1}$, *ca.* 10 times higher than that for the spontaneous decomposition of 3MBD. The average K value is $K = (7.7 \pm 0.8) \cdot 10^4\,\text{M}^{-1}$, consistent with the assumption of a rapid pre-equilibrium step. Although there exist some values for k_{DE} and K in the literature [4–7][43], no direct comparisons can be done because the employed experimental conditions and chemicals are different; however, the values obtained are of the same order of magnitude than those obtained

for the reaction of 3MBD with ascorbic acid, which also leads to the formation of an unstable transient diazo ether [4].

Bearing in mind that at the working conditions $K_{a1} \lll [H^+]$, $A \approx KK_a/[H^+]$. The obtained A values (*Table*) suggest that the product $A\,[MG_T] < 1$ when relatively low MG concentrations are employed, and under such circumstances, *Eqn. 3* predicts that k_{obs} should have an inverse dependence on acidity with a slope of unity, as it was found experimentally (*Fig. 5,b*).

Diazo ethers of the general structure ArN=NOR (R = alkyl, aryl) are rarely formed as stable products, for instance the diazo ether formally derived from naphthalen-1-ol and the benzenediazonium ion is sensitive to acid and base as well as light. Previous studies concerning the reaction of arenediazonium ions with alkoxide or phenoxide compounds, which yield diazo ethers, provide further support for the proposed mechanism but suggest that the decomposition of the diazo ether complex may not be a single step as indicated in *Scheme 4* but proceeds as indicated in *Scheme 1* [9][44 – 46]. Investigations developed by *Broxton* and *Roper* [47] confirmed that the initial reaction of ArN_2^+ ions with RO^- ions takes place in such a way that almost exclusively the (*Z*)-diazo ether is formed directly, and part of it is transformed to the (*E*)-isomer by an ionization-recombination mechanism. In recent solvolytic dediazoniation work, *Pazo-Llorente et al.* [14] concluded that the initiation pathways of the solvent-induced homolytic dediazoniations are not an electron transfer from the solvent as was believed but proceeds through the formation of a transient *O*-diazo ether in a rapid pre-equilibrium step which decomposes homolytically initiating a radical mechanism. The $Ar-N=N-O-R'$ formed may undergo subsequent isomerization to the thermodynamically stable (*E*)-isomers, which can be in some instances isolated [43], or eventually may give rise to homolytic rupture of the bonds providing the initiation of a radical process as indicated in *Scheme 1*. The bond-rotating mechanism to transform the (*Z*)- to the (*E*)-isomers has been recently described for *Sandmeyer* hydroxylations and chlorination reactions [12] but has not been extended to other systems as yet and, therefore, requires further investigations.

In conclusion, our results provide kinetic evidence consistent with the formation of an intermediate in the course of the reaction between ArN_2^+ ions and MG. The dependence of k_{obs} on acidity suggests that the reaction takes place through the ionized form of MG, leading to the formation of an unstable diazo ether intermediate. Consistent with this interpretation, saturation kinetic patterns were obtained on studying the dependence of k_{obs} on [MG]. The results obtained are surprising because it seems that the course of the reaction may be largely influenced by the position at which the first deprotonation of the trihydric phenol takes place and the availability of an activated C-atom at the *ortho* or *para* positions [12]. To the best of our knowledge, no references to this observation have been published previously in the literature or on the stability of the diazo ethers formed; further investigations with structurally similar compounds are warranted, which are in progress and will be part of future reports.

Experimental Part

Instrumentation. UV/VIS Spectra and some kinetic experiments: *Agilent-HP-8453*-UV/VIS spectrophotometer equipped with a thermostated cell carrier attached to a computer for data storage. Linear-Sweep Voltammetry: *Ecochemie-PGSTAT-10* potentiometer attached to a *663-VA Stand* (*Metrohm*) equipped with a water-jacketed voltammetry cell; three-electrode system, composed of a mercury multimode (DME, SMDE, or HMDE) working electrode, an Ag/AgCl reference electrode, and a glassy carbon rod (2×65 mm) auxiliary electrode; were recorded at constant temp. T $30 \pm 0.1°$, except where indicated.

Materials. Reagents were of maximum purity available and were used without further purification. Methyl gallate and the reagents used in the preparation of 3-methylbenzenediazonium tetrafluoroborate and in the preparation of *Britton–Robinson* (*BR*) buffer were purchased from *Fluka* or *Aldrich*. Other materials employed were from *Riedel de Häen*. All solns. were prepared with *Milli-Q* grade water. Solns. employed in electrochemical measurements were bubbled with dry N_2 (99.999%) for at least 20 min and kept under N_2 during the measurements. The *BR* buffer was prepared by mixing H_3BO_3, AcOH, and H_3PO_4, and the pH was adjusted with conc. NaOH soln. Final concentrations of the electrolytes were 0.04M. The 3MBD was prepared under nonaqueous conditions as described elsewhere [48] and stored in the dark at low temp. to minimize its decomposition. The UV/VIS spectrum of a *ca.* $1 \cdot 10^{-4}$ M aqueous buffered (pH 3) soln. of 3MBD shows a main absorption band centered at λ 250 nm and a shoulder at λ 310 nm. Variations of absorbance with [3MBD] are linear up to $2 \cdot 10^{-4}$ M, with $\varepsilon_{250} = 4700 \pm 90$ l mol^{-1} cm^{-1} and $\varepsilon_{310} = 1773 \pm 19$ l mol^{-1} cm^{-1} in keeping with literature values [39]. The UV/VIS spectrum of a $3 \cdot 10^{-4}$ M aqueous buffered (*BR*, pH 4.3) soln. of MG shows two main absorption bands centered at λ 228 ($\varepsilon_{228} = 6969 \pm 20$ l mol^{-1} cm^{-1}) and at 273 nm ($\varepsilon_{273} = 8500 \pm 15$ l mol^{-1} cm^{-1}). No significant absorbance is detected at wavelengths higher than 420 nm.

Methods. Electrochemical behavior (linear-sweep voltammetry, LSV) of solns. containing 0.1M HCl and $8.0 \cdot 10^{-5}$ M of 3MBD show two well-defined diffusion-controlled peaks, which appear at *ca.* -0.05 V (*Fig. 2,a*) and -1.2 V *vs.* Ag/AgCl (3M KCl), in agreement with [34][49][50]. Voltammograms (not shown) of HCl or buffered (*Britton–Robinson*) aq. solns. containing increasing amounts of 3MBD show that the height of both peaks increase linearly ($cc > 0.999$).

Kinetic data were obtained from electrochemical data by monitoring the decrease in the reduction peak of 3MBD at E_p *ca.* -0.05 V. The observed rate constants k_{obs} were obtained by fitting the peak current/time data to the integrated first-order *Eqn. 6* using a nonlinear least-squares method provided by a commercial computer program. Runs were done at T $30 \pm 0.1°$ under pseudofirst-order conditions, duplicate or triplicate runs gave k_{obs} values within 7%.

$$\ln\left(\frac{i_{p_t} - i_{p_\infty}}{i_{p_0} - i_{p_\infty}}\right) = -k_{obs}t \tag{6}$$

REFERENCES

[1] K. C. Brown, M. P. Doyle, *J. Org. Chem.* **1988**, *53*, 3255.
[2] K. J. Reszka, C. F. Chignell, *J. Am. Chem. Soc.* **1993**, *115*, 7752.
[3] K. J. Reszka, C. F. Chignell, *Chem.–Biol. Interact.* **1995**, *96*, 223.
[4] U. Costas-Costas, E. Gonzalez-Romero, C. Bravo Díaz, *Helv. Chim. Acta* **2001**, *84*, 632.
[5] U. Costas-Costas, C. Bravo-Díaz, E. González-Romero, *Langmuir* **2004**, *20*, 1631.
[6] U. Costas-Costas, C. Bravo-Díaz, E. González-Romero, *Langmuir* **2003**, *19*, 5197.
[7] U. Costas-Costas, C. Bravo-Díaz, E. González-Romero, *Langmuir* **2005**, *21*, 10983.
[8] A. F. Hegarty, 'Kinetics and Mechanisms of Reactions Involving Diazonium and Diazo Groups', in 'The Chemistry of Diazonium and Diazo Compounds', Ed. S. Patai, J. Wiley & Sons, NY, 1978, p. 511.

 [9] H. Zollinger, 'Diazo Chemistry I, Aromatic and Heteroaromatic Compounds', VCH, Wheinhein, Germany, 1994.
[10] P. S. J. Canning, K. McCrudden, H. Maskill, B. Sexton, *J. Chem. Soc., Perkin Trans. 2* **1999**, 2735.
[11] R. Pazo-Llorente, C. Bravo-Díaz, E. González-Romero, *Eur. J. Org. Chem.* **2003**, *17*, 3421.
[12] P. Hanson, J. R. Jones, A. B. Taylor, P. H. Walton, A. W. Timms, *J. Chem. Soc., Perkin Trans. 2* **2002**, 1135.
[13] E. González-Romero, B. Malvido-Hermelo, C. Bravo-Díaz, *Langmuir* **2002**, *18*, 46.
[14] R. Pazo-Llorente, C. Bravo-Díaz, E. González-Romero, *Eur. J. Org. Chem.* **2004**, 3221.
[15] R. Pazo-Llorente, H. Maskill, C. Bravo-Díaz, E. González-Romero, *Eur. J. Org. Chem.* **2006**, 2201.
[16] H. Zollinger, 'Color Chemistry', VCH, 1991.
[17] L.-L. Lu, X.-Y. Lu, *J. Chem. Eng. Data* **2007**, *52*, 37.
[18] I. Szele, H. Zollinger, 'Azo Coupling Reactions: Structure and Mechanism', in 'Topics in Current Chemistry', Vol. 112, 'Preparative Organic Chemistry', Vol. 112, Springer-Verlag, New York, 1983, p. 1.
[19] C. Boga, E. Del Vecchio, L. Forlani, *Eur. J. Org. Chem.* **2004**, 1567.
[20] K. H. Saunders, R. L. M. Allen, 'Aromatic Diazo Compounds', Edward Arnold, Baltimore, MD, 1985.
[21] O. Machackova, V. Sterba, K. Valter, *Collect. Czech. Chem. Commun.* **1972**, *37*, 1851.
[22] B. Zhu, X. Luo, S. Liu, *Anal. Lett.* **1997**, *30*, 963.
[23] S. G. Dmitrienko, O. M. Medvedeva, A. A. Ivanov, O. A. Shpigun, Y. A. Zolotov, *Anal. Chim. Acta* **2002**, *469*, 295.
[24] K. Gunaseelan, L. S. Romsted, E. González-Romero, C. Bravo-Díaz, *Langmuir* **2004**, *20*, 3047.
[25] K. Gunaseelan, L. S. Romsted, M. J. Pastoriza-Gallego, E. González-Romero, C. Bravo-Díaz, *Adv. Colloid. Interf. Sci.* **2006**, 303.
[26] E. N. Frankel, A. S. Meyer, *J. Sci. Food Agric.* **2000**, *80*, 1925.
[27] D. J. McClemments, E. A. Decker, *J. Food Sci.* **2000**, *65*, 1270.
[28] O. I. Aruoma, 'Free Radicals and Antioxidants in Food Science', Chapman & Hall, London, UK, 1998.
[29] D. L. Madhavi, N. R. Deshpande, D. K. Salunkhe, 'Food Antioxidants, Technological, Toxicological and Health Perspectives', Marcell Dekker, NY, 1996.
[30] J. Pokorny, N. Yanishlieva, M. Gordon, 'Antioxidants in Food: Practical Applications', CRC Press, Boca Raton, 2001.
[31] R. Chaubal, V. H. Deshpande, N. R. Deshpande, *Electron. J. Environ. Agric. Food Chem.* **2005**, *4*, 956.
[32] R. Pazo-Llorente, E. González-Romero, C. Bravo-Díaz, *Int. J. Chem. Kin.* **2000**, *32*, 210.
[33] R. Pazo-Llorente, M. C. Rodríguez-Menacho, E. González-Romero, C. Bravo-Díaz, *J. Colloid Interf. Sci.* **2002**, *248*, 169.
[34] C. Bravo-Díaz, E. González-Romero, *Electroanalysis* **2003**, *15*, 303.
[35] C. Bravo-Díaz, E. González-Romero, 'Electrochemical Behavior of Arenediazonium Ions. New Trends and Applications', in 'Current Topics in Electrochemistry', Vol. 9, Trivandrum, India, 2003.
[36] M. E. Romero-Nieto, C. Bravo-Diaz, E. Gonzalez-Romero, *Int. J. Chem. Kin.* **2000**, *32*, 419.
[37] R. Pazo-Llorente, C. Bravo-Díaz, E. González-Romero, *Fresenius J. Anal. Chem.* **2001**, *369*, 582.
[38] C. Bravo-Diaz, E. Gonzalez-Romero, *Anal. Chim. Acta* **1999**, *385*, 373.
[39] R. Pazo-Lorente, M. J. Rodriguez-Sarabia, E. Gonzalez-Romero, C. Bravo-Díaz, *Int. J. Chem. Kinet.* **1999**, *31*, 73.
[40] V. Tulyathan, R. Boulton, V. Singleton, *J. Agric. Food Chem.* **1989**, *37*, 844.
[41] N. Takenaka, M. Tanaka, K. Okitsu, H. Bandow, *J. Phys. Chem. A* **2006**, *110*, 10628.
[42] E. R. Luchkevitch, I. L. Bagal, A. V. El'tsov, *Zh. Obsch. Khim.* **1991**, *61*, 1689.
[43] M. P. Doyle, C. L. Nesloney, M. S. Shanklin, C. A. Marsh, K. C. Brown, *J. Org. Chem.* **1989**, *54*, 3785.
[44] W. J. Boyle, T. Broxton, J. F. Bunnet, *J. Chem Soc., Chem. Commun.* **1971**, 1470.
[45] J. F. Bunnet, H. Takayama, *J. Org. Chem.* **1968**, *33*, 1924.
[46] J. F. Bunnet, C. Yijima, *J. Org. Chem.* **1977**, *42*, 639.
[47] T. J. Broxton, D. L. Roper, *J. Org. Chem.* **1976**, *41*, 2157.

[48] M. C. Garcia-Meijide, C. Bravo-Díaz, L. S. Romsted, *Int. J. Chem. Kinet.* **1998**, *30*, 31.

[49] R. M. Elofson, F. F. Gadallah, *J. Org. Chem.* **1969**, *34*, 854.

[50] H. Viertler, V. L. Pardini, R. R. Vargas, 'The Electrochemistry of Triple Bond', in 'The Chemistry of Triple-Bonded Functional Groups', Supplement C, Ed. S. Patai, J. Wiley & Sons, New York, 1994, p. 583.